

Stephanie R. Wilson, MD  
Peter N. Burns, PhD  
Derek Muradali, MD  
Jessica A. Wilson, BSc  
Xiaoming Lai, PhD

**Index terms:**

Liver, US, 761.12988  
Liver neoplasms, 761.3194, 761.323,  
761.3327, 761.3328  
Liver neoplasms, US, 761.12988  
Microbubbles  
Ultrasound (US), contrast media,  
761.12988  
Ultrasound (US), harmonic study

**Radiology 2000;** 215:153–161

**Abbreviation:**

MI = mechanical index

<sup>1</sup> From the Department of Medical Imaging, Toronto General Hospital, 200 Elizabeth St, Toronto, Ontario M5G 2C4, Canada (S.R.W., D.M.), and the Department of Medical Biophysics, Sunnybrook and Women's Health Science Centre, Ontario, Canada (P.N.B., J.A.W., X.L.). From the 1998 RSNA scientific assembly. Received June 8, 1999; revision requested July 29; final revision received October 26; accepted November 2. S.R.W. and P.N.B. were supported in part by the Medical Research Council and National Cancer Institute of Canada and Mallinckrodt Medical. **Address reprint requests to** S.R.W. (e-mail: stephanie.wilson@uhn.on.ca).

© RSNA, 2000

**Author contributions:**

Guarantors of integrity of entire study, S.R.W., P.N.B.; study concepts and design, S.R.W., P.N.B.; definition of intellectual content, S.R.W., P.N.B.; literature research, S.R.W., P.N.B.; clinical studies, S.R.W., D.M.; data acquisition, X.L., J.A.W.; data analysis, J.A.W., P.N.B.; statistical analysis, P.N.B.; manuscript preparation, editing, and review, S.R.W., P.N.B.

# Harmonic Hepatic US with Microbubble Contrast Agent: Initial Experience Showing Improved Characterization of Hemangioma, Hepatocellular Carcinoma, and Metastasis<sup>1</sup>

**PURPOSE:** To characterize blood flow in focal hepatic lesions with harmonic ultrasonographic (US) imaging and a microbubble contrast agent.

**MATERIALS AND METHODS:** Thirty patients with known hepatic masses were examined after injection of a perfluorocarbon microbubble agent. Tumor vascularity was assessed with continuous, harmonic gray-scale imaging with a low mechanical index (MI). Tumor vascular volume was assessed with brief, high-MI insonation called interval-delay imaging, which caused microbubble destruction. As the total contrast agent volume in the liver reflects the total vascular volume, quantitation of lesion enhancement relative to normal hepatic enhancement helped determine the vascular volume of the tumor relative to that of normal parenchyma.

**RESULTS:** Low-MI continuous harmonic imaging showed lesional vessels in hepatocellular carcinomas, minimal or no vessels in hemangiomas, and variable vascularization in metastases. High-MI interval-delay imaging showed greater enhancement in hepatocellular carcinomas than in normal liver ( $P < .02$ ) and showed less enhancement in hemangiomas than in normal liver ( $P < .02$ ). Enhancement in metastases was greater in the margins than in the center; as a result, the lesions appeared smaller ( $P < .03$ ) and less well defined on the interval-delay images.

**CONCLUSION:** Contrast-enhanced harmonic imaging appears superior to conventional Doppler US for hepatic mass characterization. Low-MI continuous and high-MI interval-delay imaging can help assess tumor vascular pattern and microvascular volume.

Findings of a nonspecific solid mass on ultrasonographic (US) images frequently leads to computed tomographic (CT) and magnetic resonance (MR) imaging investigations, in which the use of intravascular contrast agents is routine. The characterization of hepatic masses at US traditionally has been performed without the benefit of contrast agents and has been based solely on the gray-scale morphologic features and on vascular information from color, power, and spectral Doppler US.

Unfortunately, the use of conventional Doppler US to provide vascular information often is limited by hepatic masses that are deep in the abdomen, are small, or are subject to motion artifacts from either respiratory or cardiac activity. To improve the performance of conventional US, two avenues may be pursued: The Doppler ultrasound signal can be enhanced with a contrast agent, or a recent imaging technology such as harmonic imaging can be employed.

Microbubble contrast agents for US currently are under investigation for radiologic applications. They comprise a suspension of gas bubbles whose mean size is smaller than that of a red blood cell but is sufficiently large to remain within the blood pool. They are

injected intravenously and result in echo enhancement from systemic arterial vessels of up to 30 dB (1). Contrast agents for US are unique in that they interact with the imaging process. The major determinant of this interaction is the peak negative pressure of the transmitted ultrasound pulse, reflected in the mechanical index (MI), which is indicated on the US machine. By scanning with a low transmit intensity (MI < 0.5), the bubbles of a perfluorocarbon agent can be induced into stable, nonlinear oscillation, which results in harmonic or higher-frequency echoes. It now is well established that by scanning near the maximum output power of a diagnostic US machine (MI = 1.0–1.3), microbubble contrast agents are disrupted by their acoustic oscillation. Results of *in vitro* trials show that the microbubbles in the circulation emit a strong, very brief echo as they are disrupted at high-MI insonation and show that this echo is rich in harmonics (2,3).

Conventional US machines transmit and receive ultrasound signals at the same frequency. Harmonic imaging preferentially is used to detect higher-frequency echoes, specifically those at the second harmonic. Because moving tissue does not give harmonic echoes, harmonic Doppler US shows bubbles while suppressing artifacts from tissue motion (4). With the use of a low-MI continuous technique, flow in major vessels can be detected with the resolution afforded with gray-scale imaging. Because continuous imaging takes place at a frame rate at which the interval between frames exceeds the time taken for new bubbles to wash into the scanning plane, microscopic vessels are invisible with continuous, harmonic, contrast-enhanced imaging.

In interval-delay imaging, the imaging process is interrupted for several seconds. This allows the entire vascular volume, in which the microvessels are included, to fill with contrast medium. Imaging is then commenced at a high MI. This destroys the accumulated microbubbles, which causes them to release high-intensity, nonlinear ultrasound echoes that are optimally detected by using harmonic imaging (3). It is not necessary for the bubbles to be moving for them to be detected in this way. This harmonic interval-delay method, therefore, allows the detection of blood in the capillary bed, where the flow velocity is too low to be detected with Doppler US flow techniques. In this way, harmonic gray-scale imaging can be used to detect echoes from the contrast agent when it is at very

low concentrations and when it is distributed in microscopic vessels.

Our purpose was to characterize blood flow in focal hepatic lesions with non-Doppler US harmonic imaging after the injection of a microbubble contrast agent. Low-MI continuous imaging was used to assess lesional vascularity, and high-MI interval-delay imaging was used to show the total amount of contrast agent in the vascular bed of a lesion compared with that in the surrounding normal liver, a measure of the relative vascular volume.

## MATERIALS AND METHODS

### Contrast Agent

The octafluoropropane formulation of human albumin microspheres in an injectable suspension (Optison; Mallinckrodt Medical, St Louis, Mo) is a blood pool US contrast agent comprising microbubbles that are stabilized by a protein shell. The median bubble diameter is approximately 3.5  $\mu\text{m}$ , and the concentration is  $5\text{--}8 \times 10^8$  microbubbles per milliliter. Human albumin microspheres in an octafluoropropane formulation has been approved by the U.S. Food and Drug Administration for use as a ventricular opacification agent in contrast material-enhanced echocardiography. In this study, we investigated the potential radiologic applications of the agent in hepatic diagnosis.

The protocol was approved by the Food and Drug Administration, by the Health Protection Branch of Canada, and by our institutional human studies ethics board. Informed consent was obtained from all patients.

### Contrast Material Enhancement Monitoring

The efficacy of the contrast agent was monitored quantitatively for each injection by using an independent, specially constructed Doppler US system. A single transducer was clamped and held over the femoral or brachial artery and was connected to a pulsed Doppler US system that operated at a center frequency of 5 MHz and an MI of less than 0.05. Doppler ultrasound signals were recorded digitally and were analyzed to yield a continuous estimate of the relative backscatter intensity of systemic arterial blood. This measurement was used to determine the peak intensity of the enhancement and thereby to time the interval-delay sequences. It also was used to indicate the return to

baseline intensity after the washout of the contrast agent.

### Patient Selection

Between September 1997 and July 1998, 33 patients who had a confirmed hepatic mass in one of three categories—10 with hemangioma, 12 with hepatocellular carcinoma, and 11 with metastases—were selected randomly from those referred to our US department. A confirmed diagnosis of their hepatic mass was the only inclusion criterion. Patients currently undergoing or who recently (within 30 days) underwent chemotherapy were excluded from recruitment. Informed consent was obtained from all patients.

Baseline US examinations included gray-scale, color, and power Doppler US evaluation of the lesion under study. Blood flow was classified subjectively as absent, sparse, moderate, or profuse on the basis of the number of blood vessels seen within and around the tumor.

After the baseline US examination, all patients underwent imaging after the intravenous administration of human albumin microspheres. Results in three patients were not obtained because of technical or procedural failure. Data in the remaining 30 patients were analyzed both with quantitative analysis and with blinded clinical review.

**Hemangioma.**—The 10 patients with hemangiomas included five men and five women aged 36–72 years. Diagnosis was confirmed with the results of labeled red blood cell scintigraphy in seven patients, of contrast material-enhanced CT in three patients, of serial US follow-up examinations (an unchanging lesion) for up to 10 years in three patients, and of MR imaging in one patient. Lesions ranged from 1 to 17 cm in maximal diameter. No vascularity was detected with conventional Doppler US in any lesion.

**Hepatocellular carcinoma.**—Ten patients with hepatocellular carcinoma included seven men and three women aged 34–74 years. Nine patients had histologic confirmation provided with percutaneous biopsy (three patients) or with surgery (six patients). The remaining patient had a clinical diagnosis confirmed with results of MR imaging and CT and with an  $\alpha_1$ -fetoprotein level of greater than 2,000  $\mu\text{g/L}$ . The maximal lesion diameter was 2.8–13.5 cm. Baseline Doppler US evaluation showed arterial blood flow in nine of 10 tumors, which was assessed as profuse in five, as moderate in two, and as sparse in two.

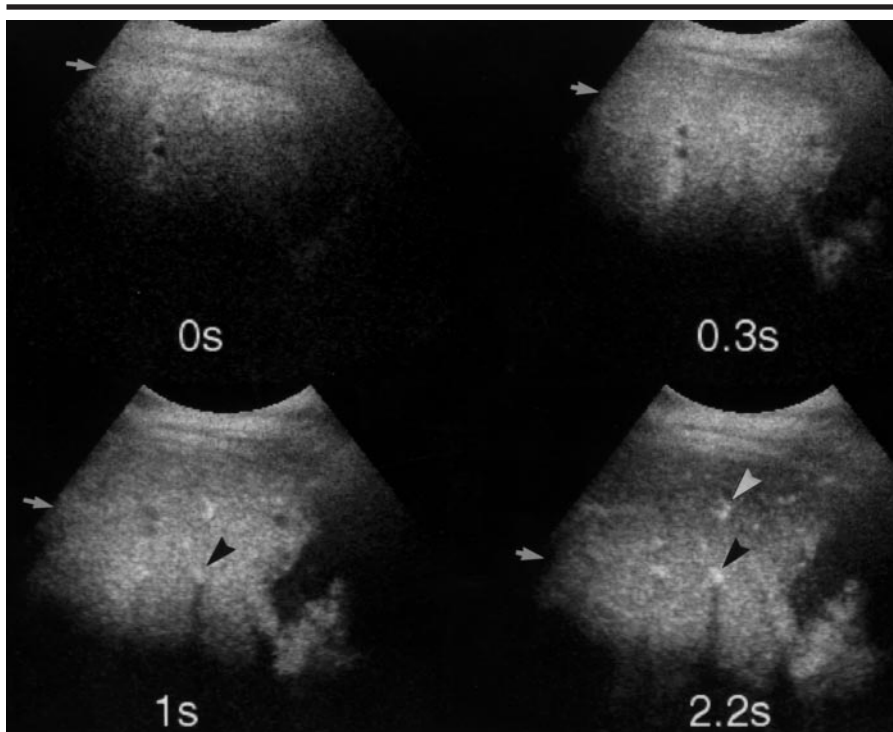


**Figure 1.** The gray-scale veil. After insonation of the liver at high MI and after injection of the contrast agent, four transverse US frames obtained through the right lobe of the liver at 0, 0.3, 1.0, and 2.2 seconds (s) show a progressive veil of increased echogenicity (arrows) that passes through the liver as the bubbles are disrupted by the ultrasound signal. There is complete bubble destruction after approximately 2 seconds of scanning. Bright echoes, some with shadowing (arrowheads), are from contrast agent-filled major hepatic vessels.

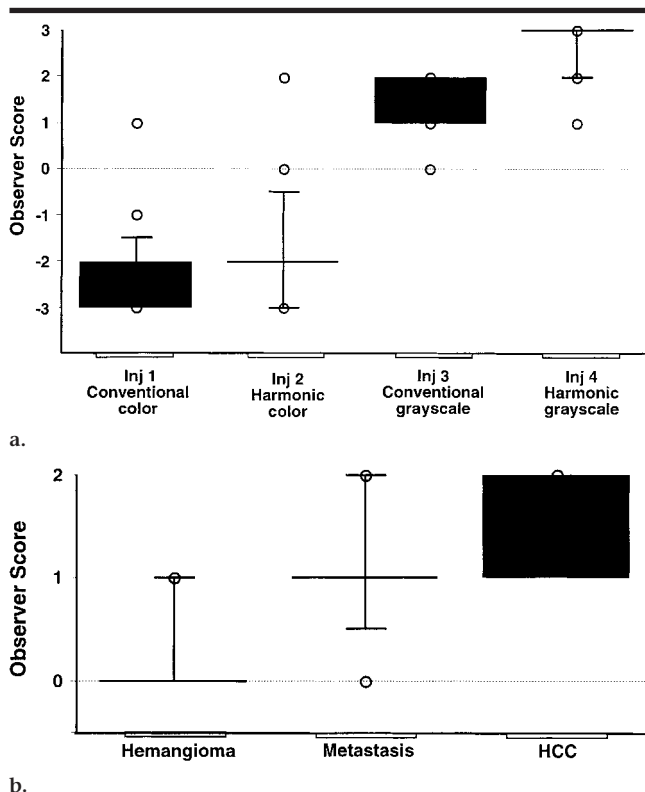


**Figure 2.** Results of the blinded reading. Box plots show the median (long horizontal line), interquartile (■), and 5th-95th-percentile ranges (short horizontal line). (a) Box plot for low-MI US imaging shows observer scores of the response to contrast agent in the four imaging modes: Negative scores indicate artifact, and positive scores indicate improved visualization of vessels. *Inj* = injection. (b) Box plot for high-MI harmonic, interval-delay US imaging shows observer scores of the participation of the three lesions that were studied in the gray-scale veil. In a and b, ○ = individual data points outside the 5%-95% range, vertical line = 5%-95% range.

**Metastases.**—Ten patients with metastases comprised eight men and two women aged 45–66 years. Primary tumors included colon cancer (seven patients), carcinoid tumor (one patient), kidney cancer (one patient), and cholangiocarcinoma (one patient). Histologic proof of the diagnosis in nine patients was obtained with percutaneous biopsy (two patients) or with surgery (seven patients). In the one patient without histologic proof of metastasis, there was overwhelming clinical evidence of disseminated malignancy and confirmatory CT scans and MR images.

Metastatic lesions ranged in maximal diameter from 1 to 12 cm. Baseline Doppler US showed moderate lesional arterial vascularity in the two lesions from vascular primary tumors (carcinoid and kidney cancer). Doppler ultrasound signals were absent on baseline studies in the remaining eight lesions.

### US Technique

All scans were obtained with HDI 3000 and 5000 scanners (ATL Ultrasound, Bothell, Wash) by using a C4-2 or C5-2 curvilinear transducer and by using prototype research software (ATL Ultrasound) for harmonic imaging. Low MIs in the range of 0.1–0.6 were selected for the blood vessel assessment, and a maximum MI of 1.3 was selected for the bubble disruption that was required for the interval-delay vascular volume assessments.

Four contrast medium injections were made with the following machine selections: injection 1, conventional color or power Doppler US; injection 2, harmonic color or power Doppler US, consistent with injection 1; injection 3, fundamental (conventional) gray-scale imaging; and injection 4, harmonic gray-scale imaging. Volumes of 2 mL were administered over approximately 1½ minutes for the Doppler US studies. Injections 3 and 4, during the gray-scale imaging sequences, were administered as 4-mL boluses.

All imaging was performed by maintaining a constant position of the transducer over the region of interest to show the lesion and to include some normal liver. For each of the four injections, imaging was divided into two components: low-MI continuous imaging and high-MI interval-delay imaging. During the delivery of the contrast agent, low-MI continuous imaging was performed to show the enhanced blood signals in both the normal hepatic blood vessels—first the hepatic artery and then the portal vein—and the lesional blood vessels,

which were assessed for their number, location, and morphology.

Vascular volume, including the arterial, venous, and capillary blood volumes in the field of view, was assessed with high-MI interval-delay imaging as follows: At the point determined with the femoral or brachial arterial Doppler ultrasound signal to be the peak of contrast medium enhancement in the systemic circulation, scanning was ceased for 5–8 seconds during a breath hold while the transducer was maintained over the lesion. Brief reinsonation caused the contrast agent bubbles that had accumulated in the microvasculature of the liver and the lesion to disrupt. In the color and power Doppler US modes, this was seen as a strong color flash throughout the region of accumulated contrast agent.

In the gray-scale fundamental and harmonic modes, on the other hand, the disruption of the bubbles occurred first in the near field, then in the midfield, and finally in the far field. The progression of the contrast agent disruption through the liver appeared as if a bright veil had been dropped through the liver (Fig 1). Freezing the imaging after the appearance of the gray-scale veil allowed for the reevaluation of the progress of the veil with a cine loop. The liver, which always contains contrast agent after an interval delay, showed increased echogenicity in the veil.

At frame-by-frame viewing, a reviewer (D.M.) blinded to the patient's name, to the medical record number, and to the diagnosis then determined the degree to which the lesion participated in the veil, as compared to the increased echogenicity of the enhancing liver at the same distance from the transducer as the lesion.

All studies were recorded on S-VHS video, with selected digital images and cine loops stored on a magneto-optical disk.

#### Analysis: Blinded Reading

Two reviewers (including D.M.) blinded to the patient's name, medical record number, diagnosis, and US findings independently scored the degree of visualized vascularity and the change in diagnostic quality of the postcontrast scan as compared with the baseline scan by using the videotaped recordings of each study. Differences in grading were then resolved with consensus. Vascularity was evaluated on images obtained with low-MI continuous imaging and was compared with that on baseline color or power Doppler US images. A score of 0 was

**TABLE 1**  
Observations of Vascular and Interval-Delay Imaging in Patients with Focal Hepatic Lesions

Lesion	Vessels at Continuous Imaging	Vascular Volume with Harmonic Gray-Scale Veil		
		Participation of Lesion	Border of Lesion	Features
Hemangioma	Absent; marginal in some cases	None	Sharp	Baseline echogenicity usually reverses in veil
Hepatocellular carcinoma	Profuse peri- and intralesional; tortuous and arborescent	Always	Sharp	White ball in veil, with black areas representing necrosis
Metastasis	Distorted, marginal	Only in margin	Diffuse	Appears smaller and poorly defined in veil

**TABLE 2**  
Quantitative Results of Interval-Delay Imaging in Patients with Focal Hepatic Lesions

Lesion	Amplitude of Lesion Echogenicity Compared with Amplitude of Hepatic Echo (dB)*		Measured Lesion Diameter Change in Veil (cm)*	
	Baseline	Veil	Transverse	Lateral
Hemangioma	2.23 ± 3.01	-3.09 ± 2.42 <sup>†</sup>	-0.3 ± 0.3	-0.2 ± 0.3
Hepatocellular carcinoma	-2.36 ± 3.22	2.80 ± 3.91 <sup>†</sup>	-0.2 ± 0.6	-0.4 ± 0.8
Metastasis	1.35 ± 3.37 (margin)	-1.72 ± 2.98 (margin)	-0.9 ± 1.3 <sup>‡</sup>	-0.8 ± 0.9 <sup>‡</sup>

\* Data are mean ± SD.  
<sup>†</sup>  $P < .02$  compared to baseline.  
<sup>‡</sup>  $P < .03$ .

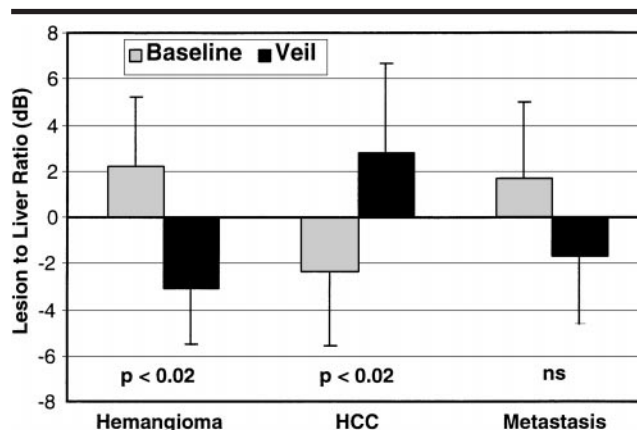


**Figure 3.** Graphic representation of the quantitative changes in the masses from baseline to the peak of the gray-scale veil. The lesion-to-liver ratio for the hemangiomas is positive at baseline, which reflects their appearance as echogenic masses. Reversal of this ratio in the veil is due to the enhancement of the surrounding normal liver in excess of the enhancement of the hemangiomas ( $P < .02$ ). Hepatocellular carcinomas (HCC), by comparison, show a negative ratio at baseline, as most of these lesions are hypoechoic relative to the background liver. Their positive ratio in the veil ( $P < .02$ ) confirms that the accumulation of microbubbles in their vascular volume is in excess of that within the normal parenchyma. The metastases are, on average, more echogenic than the liver at baseline and are less echogenic during the veil. *ns* = not significant.

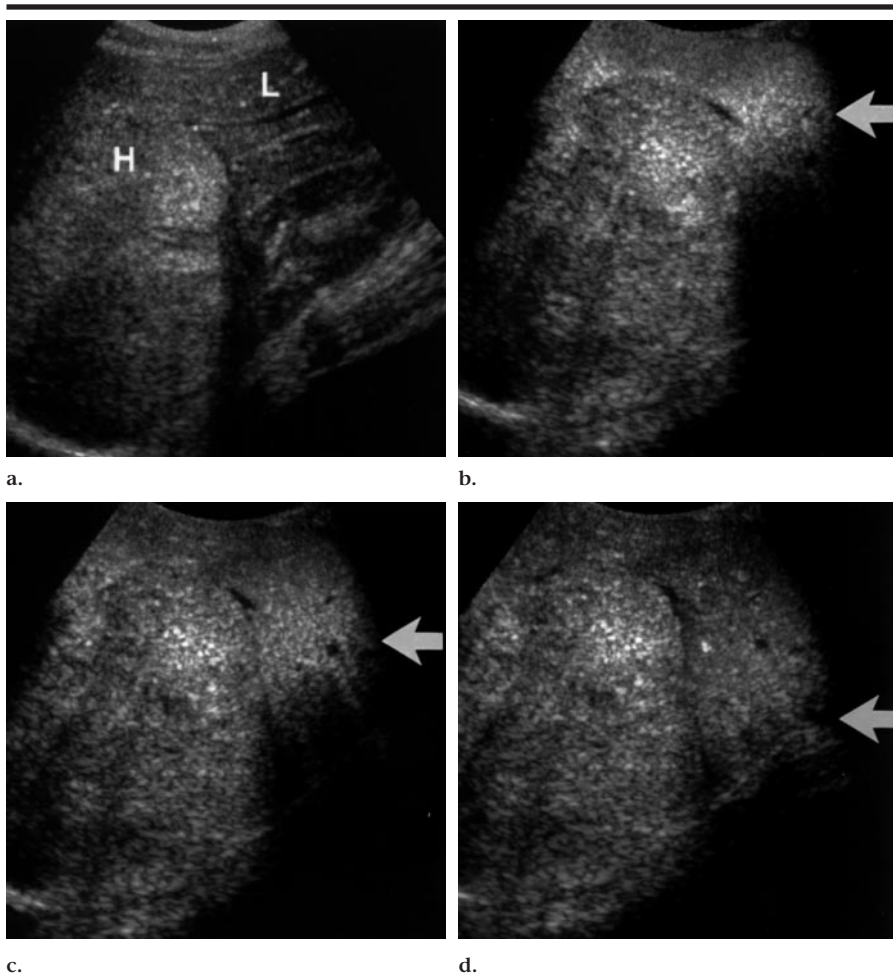


**Figure 4.** Hemangioma (*H*) vascular volume less than that of the background liver (*L*). (a) Baseline sagittal US image shows a large posterior mass of mixed echogenicity. (b–d) High-MI interval-delay US images. There is enhancement of the liver, with no participation of the hemangioma in the veil (arrows), which suggests a vascular volume less than that of the normal liver. b–d show the veil as it enhances (b) the near field, (c) the midfield, and (d) the far field.

assigned if there was no change in vessel assessment from baseline imaging; 1, for sparse vascularity not seen at baseline imaging; 2, for moderate vascularity not seen at baseline imaging; and 3, for profuse vascularity not seen at baseline imaging. Because vascularity assessment is inversely affected by artifacts, we assigned a score of –1 for mild artifacts, –2 for moderate artifacts, and –3 for severe artifacts with reduced image quality.

Qualitative vascular volume assessment was performed on images of the gray-scale veil obtained with the high-MI interval-delay technique. A score of 0 was assigned if there was little or no participation of the lesion in the veil; a score of 1, if there was participation of the lesion margin in the veil; a score of 2, if there was participation of the lesion equal to that of the normal liver; and a

score of 3, if there was participation of the lesion in excess of that of the normal liver.

#### Analysis: Quantitative

The apparent size of the lesion on a baseline image was compared with the apparent size of the lesion on a harmonic gray-scale image obtained during injection 4 that showed the peak of the gray-scale veil at the same depth from the transducer as the lesion. These images were selected by consensus by S.R.W. and P.N.B. The maximal lesion diameters on these two images were measured and compared by a single observer (J.A.W.).

On the same pre- and postinjection images, regions of interest were placed in the tumor mass and in the normal hepatic parenchyma at the same depth. By using knowledge of the display dynamic

range and the gray-scale map, these regions were transformed on a pixel-by-pixel basis to their corresponding echo levels. Research software (HDI LAB; ATL Ultrasound) was used to derive a mean echo amplitude and SD for each region of interest. From these data, a mean echo amplitude of the lesion relative to the normal liver was calculated. This value corresponded to the relative amplitude of the detected echo and was independent of instrument display parameters such as the gray-scale map.

Where the lesion appearance was heterogeneous within the veil, as was the case for the metastases, the region of interest included the entire lesion. The mean echo level of the lesion was compared with that of the surrounding parenchyma in each of the three lesion types before and after the administration of the contrast agent. The difference between the two measurements was assessed by using the Student *t* test and the Wilcoxon signed rank test.

From the data recorded by using the pulsed Doppler US arterial monitor, time-response curves of the contrast medium injections were produced by using a linear analysis method that provided a measure of the backscatter enhancement in the systemic arterial circulation without destroying the bubbles. The method and its validation are described elsewhere (5). The following measures of enhancement were calculated from these curves: the peak enhancement intensity (in decibels), the duration of enhancement (in minutes), and the time to peak enhancement (in seconds).

## RESULTS

In the 120 injections in the 30 patients, enhancement of large vessels was seen in all patients, and substantial blood pool enhancement from the femoral or brachial artery was recorded with the Doppler US monitor. It showed a mean peak enhancement due to the agent of  $24 \text{ dB} \pm 5$  (SD), with a mean duration of 7.5 minutes  $\pm 2.1$  for slow injections and of 4.2 minutes  $\pm 1.6$  for bolus injections. The mean time to peak enhancement for the bolus injections was 37.4 seconds  $\pm 25.1$ .

In all but four of the 30 patients, the veil was imaged adequately for quantitative analysis. The four patients with incomplete imaging underwent technically demanding examinations that required suspended respiration for the lesion to be maintained in the field of view.

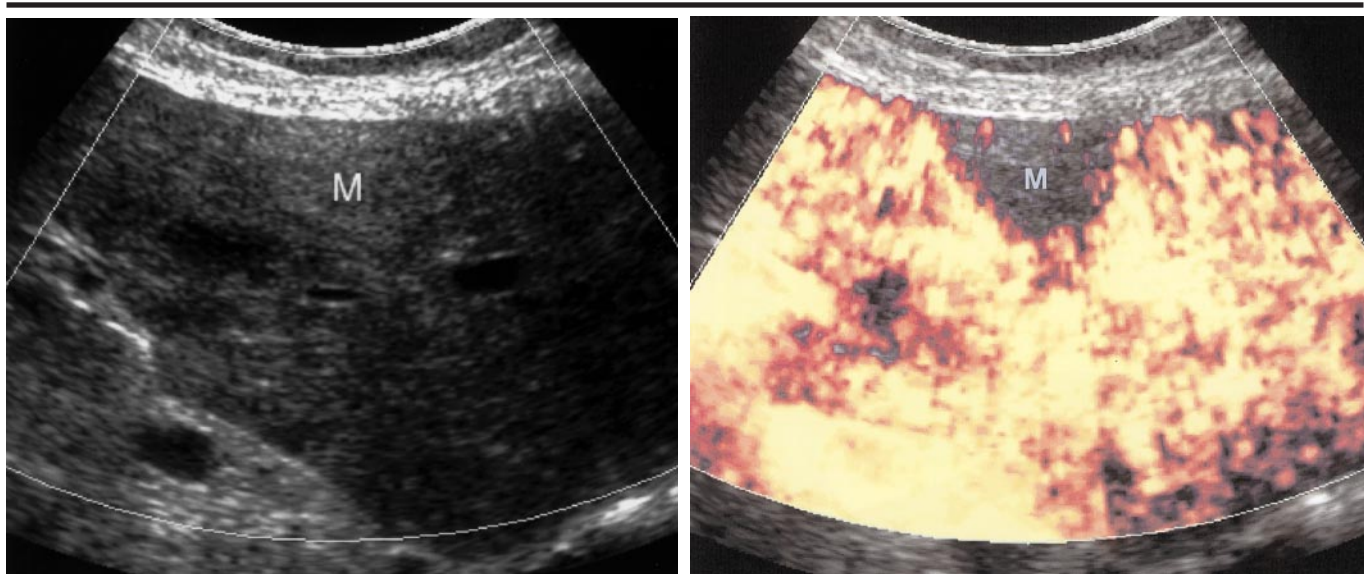


**Figure 5.** Power flash through a hemangioma, with vascular volume signal less than that of the background liver. (a) Baseline transverse US image of the left lobe of the liver shows that the mass (*M*) is slightly more echogenic than the adjacent normal liver. (b) High-MI interval-delay US image shows the power flash. After an interval delay with a brief cessation of scanning, the hepatic parenchymal flash occurs at a lower threshold than that of the lesion. The liver, filled with contrast agent, shows diffuse signal, whereas the hemangioma (*M*) appears as a void.

The contrast agent proved easy to handle and was stable and tolerated well by all patients. No (major or minor) adverse events associated with the administration of contrast agent were observed.

### Blinded Review

The results of the blinded review are shown in Figure 2a. Injection 1, in which the contrast agent was used as a simple echo enhancer in conventional color or power Doppler US, resulted in the deterioration of the diagnostic quality of the images in 29 of the 30 (97%) patients, with 18 (60%) patients having images judged to show severe artifacts. The color and power Doppler US modes had a severe blooming artifact and saturation of the color box, with no interpretable information.

In injection 2, the addition of harmonic imaging to the color and power Doppler US modes reduced artifacts and improved sensitivity on US images in 13 of 30 (43%) patients, but moderate artifacts still were seen on US images in 16 of 30 (53%) patients and severe artifacts were seen on US images in seven of 30 (23%) patients.

After injection 3, for which conventional gray-scale imaging was used, we detected some vascularity in 29 of 30 (97%) patients but detected profuse vessels in none (0%) and failed to detect the agent's presence at all in one (3%) patient.

The same dose was given in injection 4, for which harmonic gray-scale imaging was performed, and 29 of 30 (97%) patients showed improved visualization of vascularity over that with conventional imaging, with 23 of 30 (77%) showing profuse patterns not seen on the baseline images. Harmonic gray-scale imaging also improved structural contrast in the image, although it frequently was associated with deterioration in image resolution.

### Lesion-Specific Findings

The findings for the three classes of tumor are summarized descriptively in Table 1; the quantitative measurements are shown in Table 2 and in Figure 3.

**Hemangiomas.**—Hemangiomas showed sharply defined borders on baseline images and after injections (Figs 4, 5). After injection, no intralesional vessels were delineated in five patients, with sparse marginal vascularity shown in four others. The remaining patient had an indeterminate assessment of vessels. The blinded reader (Fig 2b) found no participation of the hemangioma in the color flash or in the gray-scale veil at interval delay in eight of 10 patients (Figs 4b, 5b). On interval-delay images, harmonic gray-scale veils were clearer than the flash produced with harmonic color and power Doppler US.

**Hepatocellular carcinoma.**—Consistent findings of hepatocellular carcinoma were

shown by using continuous low-MI harmonic imaging with contrast agent enhancement. Good delineation of both perilesional and intralesional blood vessels revealed an extensive arborescent pattern within the tumors (Fig 6b). The blinded reader found participation of the hepatocellular carcinoma in the veil in 10 of 10 patients.

It was found that high-MI interval-delay scans produced a color flash (Fig 6e) or a gray-scale veil (Fig 6c) whose brightness was equal to (in one patient) or was in excess of (in nine patients) that of normal liver. At the peak of the veil, the tumor appeared most frequently as a white ball (Fig 6c) against a less echogenic liver regardless of its baseline appearance.

**Metastases.**—The metastases from the colon showed variable echogenicity at baseline imaging (Fig 7,A). On low-MI continuous, harmonic gray-scale postcontrast images, small circumferential vessels were seen around the lesion, with irregular, penetrating branches that coursed toward the lesion center (Fig 7,B).

On high-MI interval-delay images, the lesion centers showed less echogenicity than normal liver, whereas the margin of the tumor participated in the veil. The result was that the lesions appeared smaller and less well defined than on baseline images, often with their echogenicity reversed relative to the echogenicity of the normal liver (Fig 7,C). In seven of the 10 patients, only the margin

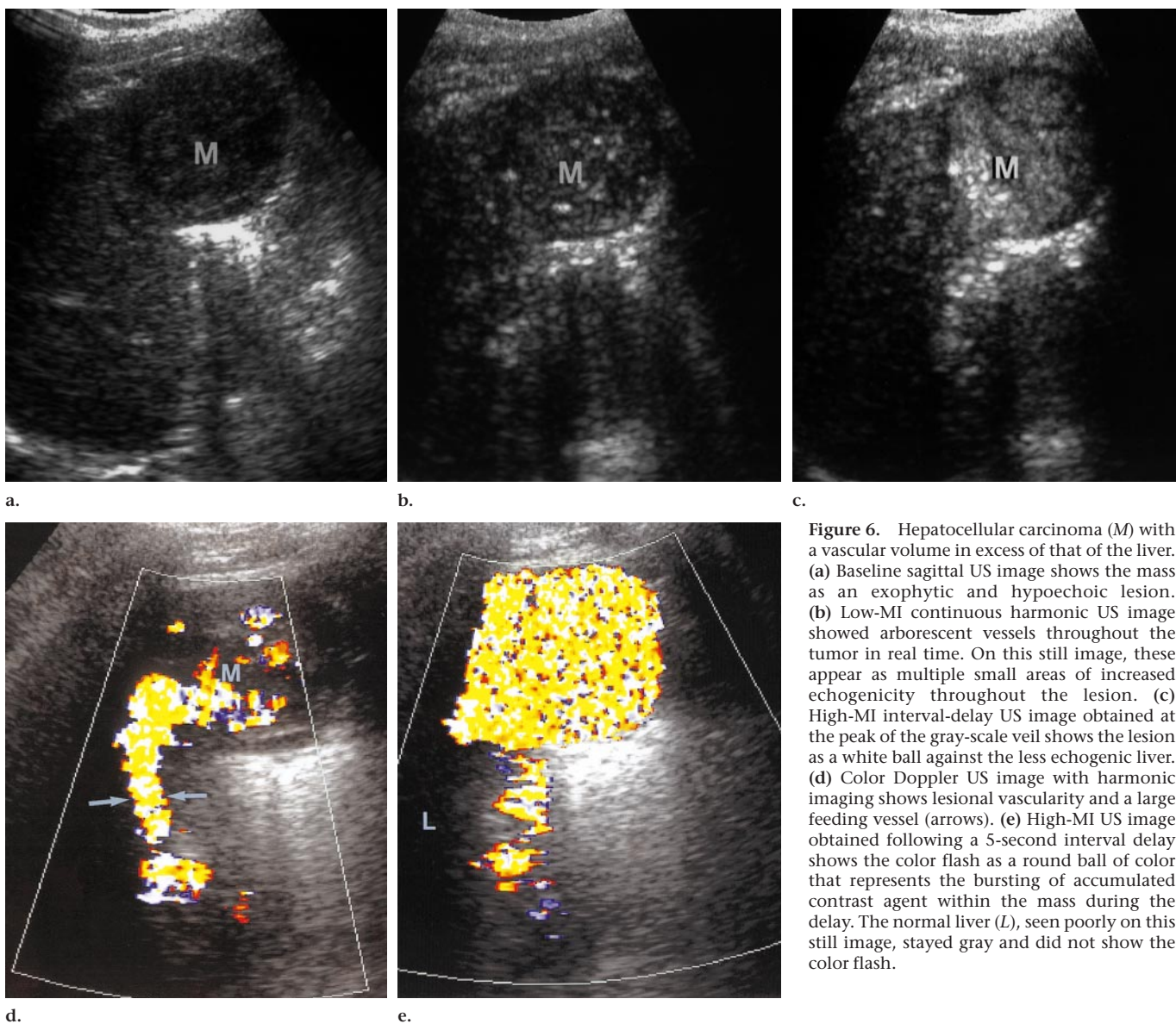


**Figure 6.** Hepatocellular carcinoma (*M*) with a vascular volume in excess of that of the liver. (a) Baseline sagittal US image shows the mass as an exophytic and hypoechoic lesion. (b) Low-MI continuous harmonic US image showed arborescent vessels throughout the tumor in real time. On this still image, these appear as multiple small areas of increased echogenicity throughout the lesion. (c) High-MI interval-delay US image obtained at the peak of the gray-scale veil shows the lesion as a white ball against the less echogenic liver. (d) Color Doppler US image with harmonic imaging shows lesional vascularity and a large feeding vessel (arrows). (e) High-MI US image obtained following a 5-second interval delay shows the color flash as a round ball of color that represents the bursting of accumulated contrast agent within the mass during the delay. The normal liver (*L*), seen poorly on this still image, stayed gray and did not show the color flash.

participated in the veil; in two patients, both with vascular metastases, all of the lesion participated; and in one patient, none of the lesion participated. The two patients with vascular metastases (renal and carcinoid primary tumors) had marked lesional vascularity, but without the tortuosity and arborescent pattern seen with hepatocellular carcinoma.

### Quantitative Measurements

The quantitative results of the measurement of the echogenicity of each hepatic lesion relative to the parenchyma both before and during the veil are shown in Table 2 and are shown graphically in Figure 2.

The measurements show that, on average, the hemangiomas were 2.23 dB more echogenic than normal liver at baseline imaging. In the harmonic gray-scale veil, however, the same lesions were on average 3.09 dB less echogenic than the surrounding liver, as the liver enhanced in excess of the hemangiomas.

The hepatocellular carcinomas, in comparison, were seen as hypoechoic masses at baseline imaging (mean echogenicity,  $-2.36$  dB with respect to the liver) but were brighter than the liver during the veil (mean echogenicity, 2.80 dB). Both these differences from baseline imaging were significant ( $P < .02$ ).

On average, the gray-scale veil reduced the echogenicity of the metastases with respect to the liver, which reflected

the greater enhancement of the normal parenchyma with the contrast medium. These differences were not statistically significant, however, and reflected the highly variable appearance of metastasis at baseline scanning. However, the metastases were measured consistently to have a smaller apparent diameter during the veil than at baseline imaging ( $P < .03$ ), which reflected the participation of the periphery or of the margin of the tumor in the veil.

### DISCUSSION

Knowledge of the vascularity of a hepatic mass is essential to determine the nature of the mass. To this end, CT and MR

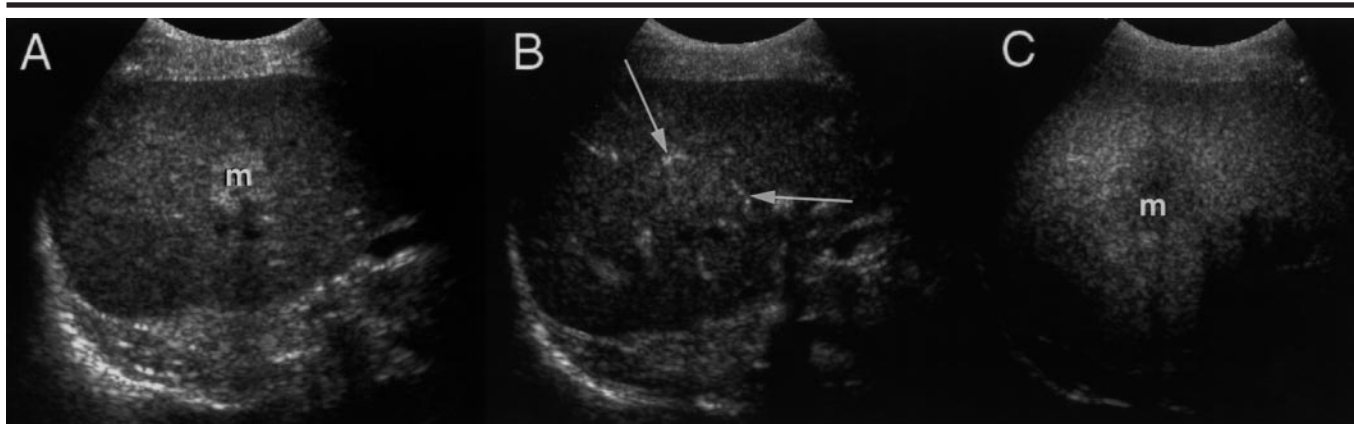


**Figure 7.** Metastasis from colon cancer. *A*, Baseline sagittal US image shows that the mass (*m*) is inhomogeneous but mainly increased in echogenicity as compared with the background normal liver. *B*, Low-MI continuous US image shows small vessels (arrows) that course from the periphery toward the lesion center. *C*, High-MI interval-delay US image for vascular volume assessment at the peak of the gray-scale veil shows that the mass (*m*) appears smaller and poorly defined. Echogenicity is reversed as the liver enhances in excess of the lesion. The apparent decrease in lesion size is attributed to the enhancement of the lesion periphery.

imaging are performed regularly with contrast agents by using different methods of administration and by using different imaging sequences to optimize vascular information. US contrast agents for medical imaging only recently have become available for clinical use. Although they have been approved for echocardiography and for the enhancement of Doppler ultrasound signals, to our knowledge, applications in the liver are still under clinical investigation (6–11).

To our knowledge, most studies of contrast agents in the liver reported on to date have been limited by the use of conventional gray-scale and Doppler US technology. Our experience shows that simply adding contrast agents in conventional color and power Doppler US imaging actually reduces the diagnostic utility of the examination. Images from such examinations show extensive color blooming and saturation of the color box, artifacts that obscure appreciation of the enhancement of Doppler ultrasound signals from the tumor vessels.

It is the application of harmonic imaging that greatly improves the options for hepatic mass evaluation with contrast agents. To image the contrast agent in blood vessels without destroying the bubbles, a low MI must be used, which reduces the sensitivity of the image. In spite of this, low-MI continuous harmonic imaging reveals vessels not seen by using conventional Doppler US modes, with or without contrast material enhancement. One reason for this is the absence of motion artifacts with the contrast-enhanced harmonic approach. At blinded review, the harmonic gray-scale images consistently showed the fewest

artifacts and showed the most evidence of lesional vascularity. Furthermore, the resolution afforded on the harmonic gray-scale images was superior to that on color and power Doppler US images, in which blooming made the vessels appear much larger than they actually were.

The gray-scale veil, descending throughout the liver with high-MI interval-delay imaging, is a consequence of bubble destruction, which occurs when the peak intensity of the ultrasound beam exceeds a critical peak pressure value (which corresponds to an MI of approximately 1.0) that disrupts the bubble. Because the disrupting bubbles attenuate the ultrasound intensity, those carried in superficial tissue “shield” the bubbles more distally during the first imaging frame. That frame shows a bright band as the superficial bubbles are disrupted. The second frame then disrupts the band beneath, and so on, until the bubbles in the entire field of view are destroyed and the veil has descended to the distal portion of the perfused organ.

The intensity of the echo that produces the ultrasound veil is proportional to the intensity of the backscattered echo from the bubbles, which has been shown to be proportional to the number of microbubbles present within the ultrasound beam (12). As the bubbles carried in the vascular system are too large to diffuse outside the vascular space, this signal level is then related directly to the total vascular volume within the scanning plane. This measurement requires the use of microbubble contrast agents and harmonic imaging and offers information not previously available with US.

To assess the vascular volume of a hepatic lesion relative to that of the sur-

rounding parenchyma, this echo level was measured simply in two regions of interest, one in the lesion and one in the liver, at equal depths from the transducer. These measurements were made from the echo signal itself and were independent of the postprocessing map used to create the video image.

A high-vascular-volume lesion appears as white or as whiter than the adjacent parenchyma, whereas an avascular lesion appears less white or even black relative to the adjacent enhancing normal hepatic parenchyma. The quantitative measurements in Table 2 confirm this. Thus, a hepatocellular carcinoma that is echo poor relative to the surrounding liver on baseline images becomes echogenic during the veil (Fig 6c); a hemangioma that is echogenic relative to the surrounding liver on baseline images becomes echo poor during the veil (Fig 4b–4d). This reversal in echogenicity was statistically significant for both lesions, as shown in Table 2.

These lesion-specific observations suggest that the hepatocellular carcinomas have a vascular volume in excess of that of the normal liver, whereas the hemangiomas have a vascular volume less than that of the normal liver. These observations may appear inconsistent with those from contrast-enhanced CT and MR imaging, in which, for example, a hemangioma is seen to opacify slowly from the margin to the center with time.

However, unlike the CT and MR imaging contrast agents, which diffuse through the permeable vascular endothelium, US contrast agent microbubbles stay within the vascular space, and their number reflects its volume. After many minutes, these agents remain within the blood

pool, even in cancers, in which changes in vascular permeability are commonly associated with tumor angiogenesis (13,14). For this reason, we do not believe that the results of this study should be compared directly with the findings of CT and MR imaging studies of focal hepatic lesions.

The limitations of this preliminary study must be appreciated. We restricted inclusion of patients to those with the three most commonly encountered hepatic masses—metastatic disease, hemanangioma, and hepatocellular carcinoma. In this study, the diagnosis of the lesions was made before the inclusion of patients. The overall number of patients in each category was small, and the emphasis on colorectal primary carcinoma for the metastatic tumor group reflects the demographics at our institution.

Hepatic mass evaluation with US contrast agents is in its infancy. Harmonic US imaging with microbubble contrast material can be used to assess both the tumor vessel morphology with low-MI continuous imaging and the relative microvascular volume of the tumor with high-MI interval-delay imaging. We believe this success is related to the superior resolution and artifact reduction of harmonic gray-scale imaging compared with that of conventional color and power Doppler US, contrast material enhanced or not.

The results of this small study are promising and suggest the potential to differentiate hepatic tumors on the basis of their appearance and response to US contrast agents; however, the specific vascular features of each tumor group need to be validated in a much larger prospective trial.

#### References

1. Burns PN, Powers JE. Optimising ultrasound imaging instruments for contrast agents. In: Nanda NC, Schlieff R, eds. *Advances in echo imaging using contrast enhancement*. Vol 2. Amsterdam, the Netherlands: Kluwer, 1997; 139–170.
2. Burns PN, Wilson SR, Muradali D, Powers JE, Greener Y. Microbubble destruction is the origin of harmonic signals from FS069 (abstr). *Radiology* 1996; 201(P):158.
3. Porter TR, Xie F, Kricsfeld D, Armbruster RW. Improved myocardial contrast with second harmonic transient ultrasound response imaging in humans using intravenous perfluorocarbon-exposed sonicated dextrose albumin. *J Am Coll Cardiol* 1996; 27:1497–1501.
4. Burns PN, Powers JE, Hope Simpson D, Uhlendorf V, Fritzsche T. Harmonic imaging: principles and preliminary results. *Angiology* 1996; 47:63–73.
5. Burns PN, Liu JB, Hilpert P, Goldberg BB. Intravenous US contrast agent for tumor diagnosis: quantitative studies (abstr). *Radiology* 1990; 177(P):140.
6. Tanaka S, Kitamura T, Numata K. Color Doppler flow imaging of liver tumors. *AJR Am J Roentgenol* 1990; 154:509–514.
7. Hosten N, Puls R, Lemke AJ, et al. Contrast enhanced power Doppler sonography: improved detection of characteristic flow patterns in focal liver lesions. *J Clin Ultrasound* 1999; 27:107–115.
8. Uggowitz M, Kugler C, Groll R, et al. Sonographic evaluation of focal nodular hyperplasia (FNH) of the liver with a transpulmonary contrast agent (Levovist). *Br J Radiol* 1998; 71:1026–1032.
9. Pennisi F, Farina R, Politi G, Lombardo R, Puelo S. Hepatic focal lesions: role of color Doppler ultrasonography with contrast media. *Radiol Med (Torino)* 1998; 96:579–587. [Italian]
10. Ernst H, Hahn EG, Balzer T, Schlieff R, Heyder N. Color Doppler ultrasound of liver lesions: signal enhancement after intravenous injection of the ultrasound contrast agent Levovist. *J Clin Ultrasound* 1996; 24:31–35.
11. Kim AY, Choi BI, Kim TK, et al. Hepatocellular carcinoma: power Doppler US with a contrast agent—preliminary results. *Radiology* 1998; 209:135–140.
12. Schwarz KQ, Bezante GP, Chen X, Mottley JG, Schlieff R. Volumetric arterial flow quantification using echo contrast: an in vitro comparison of three ultrasonic intensity methods—radiofrequency, video, and Doppler. *Ultrasound Med Biol* 1993; 19:447–460.
13. Dvorak HF, Brown LF, Detmar M, Dvorak AM. Vascular permeability factor: vascular endothelial growth factor, microvascular hyperpermeability, and angiogenesis. *Am J Pathol* 1995; 146:1029–1039.
14. Su MY, Najafi A, Nalcioğlu O. Regional comparison of tumour vascularity and permeability measured by albumin-Gd-DTPA and Gd-DTPA. *Magn Reson Med* 1995; 34:402–411.